nature climate change

LETTERS

PUBLISHED ONLINE: 27 FEBRUARY 2017 | DOI: 10.1038/NCLIMATE3220

Aerosol-weakened summer monsoons decrease lake fertilization on the Chinese Loess Plateau

Jianbao Liu[1,2], Kathleen M. Rühland[3], Jianhui Chen[1], Yangyang Xu[4], Shengqian Chen[1], Qiaomei Chen[1], Wei Huang[1], Qinghai Xu[5], Fahu Chen[1,2]* and John P. Smol[3]*

Anthropogenic aerosol increases over the past few decades have weakened the Asian summer monsoon[1–3] with potentially far-reaching socio-economic and ecological repercussions. However, it is unknown how these changes will affect freshwater ecosystems that are important to densely populated regions of Asia. High-resolution diatom records and other proxy data archived in lake sediment cores from the Chinese Loess Plateau allow the comparison of summer monsoon intensity, lake trophic status and aquatic ecosystem responses during warming periods over the past two millennia. Here we show that an abrupt shift towards eutrophic limnological conditions coincided with historical warming episodes[4,5], marked by increased wind intensity and summer monsoon rainfall leading to phosphorus-laden soil erosion and natural lake fertilization. In contrast, aerosol-affected Anthropocene warming catalysed a marked weakening in summer monsoon intensity leading to decreases in soil erosion and lake mixing. The recent warm period triggered a strikingly different aquatic ecosystem response with a limnological regime shift marked by turnover in diatom species composition now dominated by oligotrophic taxa, consistent with reductions in nutrient fertilization, reduced ice cover and increased thermal stratification[6]. Anthropogenic aerosols have altered climate–monsoon dynamics that are unparalleled in the past ~2,000 years, ushering in a new ecological state.

The Chinese Loess Plateau (CLP) is the cradle of Chinese civilization, and environmental changes in this region have influenced the historical trajectory of ancient China[7]. The CLP is the largest loess region in the world in terms of extent, thickness and depositional sequence, and covers a total area of 640,000 km^2 (ref. 8). The more than 100 million people living on the CLP are faced with the world's most serious erosion issues, particularly large losses in soil nutrients[7,8].

The climate of the CLP is largely influenced by the Asian monsoon circulation (Fig. 1a), and its location at the monsoon boundary zone makes the CLP particularly sensitive to global climate change[9]. More than 70% of the annual precipitation in the CLP falls in intense storms during the summer monsoons between June and September, and can cause extreme soil erosion[8,10] (Fig. 1b). This eroded surface soil delivers a massive amount of soil phosphorus (P) (40 million tons/year) into lakes, reservoirs and river systems such as the Yellow River (Fig. 1b), and ultimately into the marine ecosystem (Supplementary Fig. 1), resulting in severe eutrophication problems[11]. Importantly, the middle and lower reaches of the Yellow River are major sources of fresh water for about 107 million people, and often referred to as 'the Mother River of China'. The pollution and eutrophication of the Yellow River, whose sediment discharge from erosion exceeds the combined discharges of the Nile and Amazon rivers[12], directly influences the livelihood of this large population[11].

Recent studies have convincingly argued that increases in anthropogenic aerosols play an important role in affecting Asian summer monsoon intensity[1,3,13–16] that will have significant implications for more than a third of the world's population. Changes to the monsoon system have tremendous impacts on agriculture, health, water resources, economies, and ecosystems throughout Asia, as monsoon rains provide up to 80% of the region's annual mean precipitation. However, it is unknown how reductions in monsoon intensity can affect freshwater ecosystems that are important to a large portion of the Asian population. Here, we use well-dated, high-resolution palaeolimnological records from a remote alpine lake (Lake Gonghai) on the CLP to compare lake responses to major periods of past and present climate warming over the past two millennia. This approach offers an excellent 'time window' for making comparisons between the complexities of recent anthropogenic climate change with well-documented past warm periods in this region[17], both in terms of forcing mechanisms and the response of aquatic ecosystems.

Unlike major warming periods in the past, recent anthropogenic climate change is further complicated by interactions with multiple anthropogenic forcings, including greenhouse gases, anthropogenic aerosols, and land-use changes. Rapid economic growth, industrialization and urbanization in developing Asian countries has led to severe air pollution over the past few decades, resulting in Asia becoming a major source of aerosol emissions and an important contributor to global climate change[18]. This rapid and pronounced increase in anthropogenic aerosols has been linked to the widespread decrease in summer monsoon rainfall and wind intensity over Asia[1,3,13,14]. Specifically, changes in incoming solar radiation forced by anthropogenic aerosols have reduced the thermal contrast between the Asian continent and the Indian and Pacific oceans, and thus the monsoonal circulation[15,16].

Lake Gonghai (38° 54′ N, 112° 14′ E; 1,840 m above mean sea level) is a freshwater alpine lake located on the CLP (Supplementary Fig. 1a). This remote, high-elevation lake was strategically chosen to be representative of the region as it is a hydrologically closed, simple basin with a small, undisturbed catchment, and therefore an excellent passive monitor of environmental and

[1]Key Laboratory of West China's Environmental System (Ministry of Education), College of Earth and Environmental Sciences, Lanzhou University, Lanzhou 730000, China. [2]CAS Center for Excellence in Tibetan Plateau Earth Sciences of the Chinese Academy of Sciences, Beijing 100101, China. [3]Paleoecological Environmental Assessment and Research Lab (PEARL), Department of Biology, Queen's University, Kingston, Ontario K7L 3N6, Canada. [4]Department of Atmospheric Science, Texas A&M University, College Station, Texas 77842, USA. [5]Institute of Nihewan Archaeology Research, College of Resources and Environment, Hebei Normal University, Shijiazhuang 050024, China. *e-mail: fhchen@lzu.edu.cn; smolj@queensu.ca

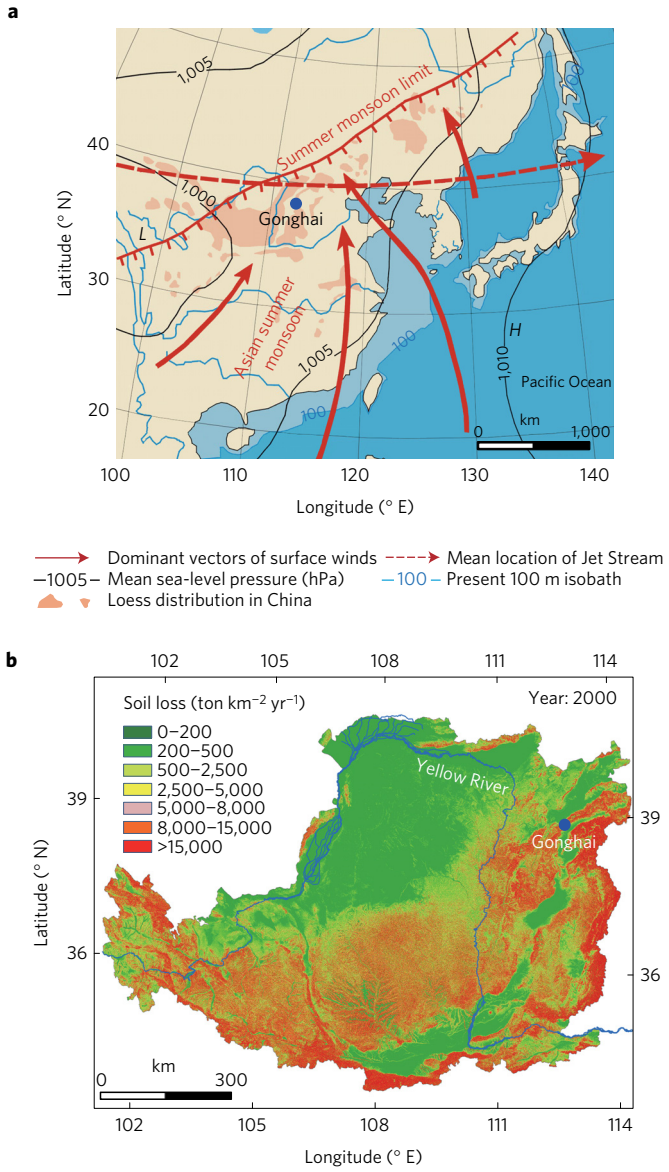

Figure 1 | Lake Gonghai, located at the CLP, considered to be the most erodible area on Earth, is largely influenced by the Asian summer monsoon. a, Climate system of the Asian monsoon area[30]. Summer monsoon rainfall and wind-dominated Asian summer monsoon region. **b**, Distribution of soil loss (ton km^{-2} yr^{-1}) on the CLP[31]: the erosion modulus of most regions on the CLP is above 8,000 ton km^{-2} yr^{-1}. The blue dot indicates the location of Lake Gonghai. Also shown is the Yellow River system (blue line).

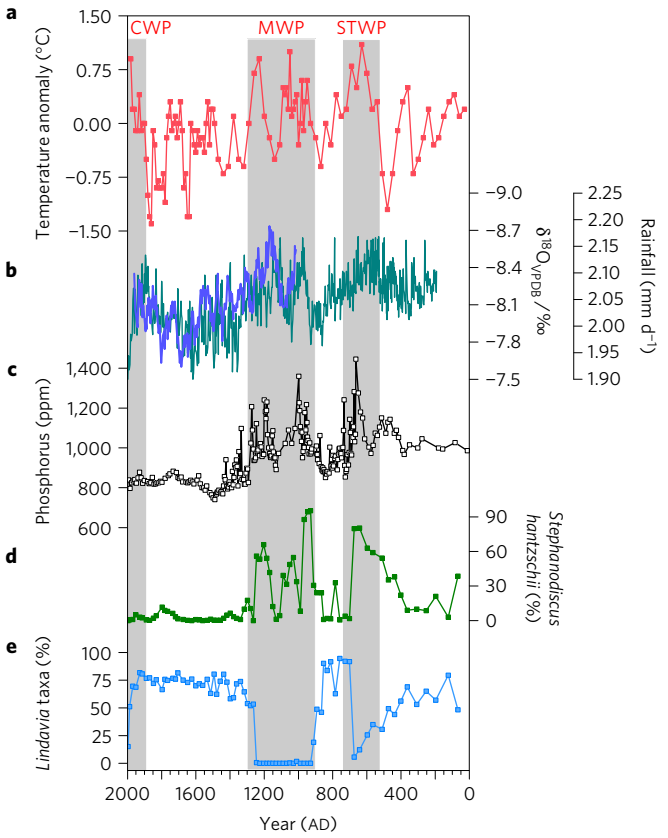

Figure 2 | Long-term trends (over the past ~2,000 years) in reconstructed air temperature and Asia summer monsoon rainfall compared with the Lake Gonghai sediment core trends for phosphorus-laden soil erosion, and shifts in dominance between oligotrophic (low nutrient) and eutrophic (high nutrient) diatom indicators. a, Air temperature reconstructed from phenological observations recorded in Chinese historical documents from North China[28]. **b**, Reconstruction of Asian summer monsoon rainfall from speleothem $\delta^{18}O$ records from Wanxiang Cave and Huangye Cave (dark cyan line)[24,25] and the modelled Asian summer monsoon rainfall from the ECHO-G model simulation[26] (blue line). **c**, Trends in the concentration of sediment phosphorus determined from the Lake Gonghai core. **d**, Changes in the relative abundances of the diatom taxon *Stephanodiscus hantzschii*, a well-documented eutrophic indicator. **e**, Relative abundances of *Lindavia* taxa (*L. praetermissa* and *L. bodanica*), diatoms characteristic of low nutrient concentrations. Grey shading corresponds to the three warm periods recognized over the past ~2,000 years in China including the Sui–Tang Warm Period (STWP), the Medieval Warm Period (MWP) and the Current Warm Period (CWP).

climatic change. The lake has a surface area of ~0.36 km^2 with a maximum water depth of ~10 m and a flat lake bed, making it an ideal palaeolimnological study site (Supplementary Fig. 1b,c). Importantly, the lake is remote and minimally affected by local human activities. Lake Gonghai in the CLP was also strategically chosen for this study as it is located within a region that is relatively low in atmospheric nitrogen deposition[19]. Furthermore, Lake Gonghai is currently oligotrophic (mean concentration values for total phosphorus (TP) and total nitrogen (TN) are 9.84 and 398 μg l^{-1}, respectively) and is strongly phosphorus limited (TN:TP mass ratio = 40.5). The lake's strategic location and limnological characteristics preclude it from being strongly affected by the recent increases in global atmospheric nitrogen deposition. The monthly mean temperature in this region ranges between −14 °C and +23 °C. The lake is currently typically ice covered from the middle of November to the end of April. The Lake Gonghai region has recently experienced large-magnitude increases in air temperature[20] that are consistent with the amplification of warming reported in high-mountain regions[21].

Here we use high-resolution diatom records from two dated Lake Gonghai sediment cores to determine how recent aerosol-driven anthropogenic climate change compares with past episodes of natural warming in terms of summer monsoon intensity, lake fertilization, and aquatic ecosystem dynamics. We reconstruct past limnological conditions mainly using changes in diatom (Bacillariophyceae) assemblage composition. Diatoms are well-documented indicators of lake water nutrient levels[22] and have also been widely used to track changes in climate-related lake properties, such as the extent of lake ice and thermal stratification[6]. By their nature, palaeolimnological records typically integrate ecological signals

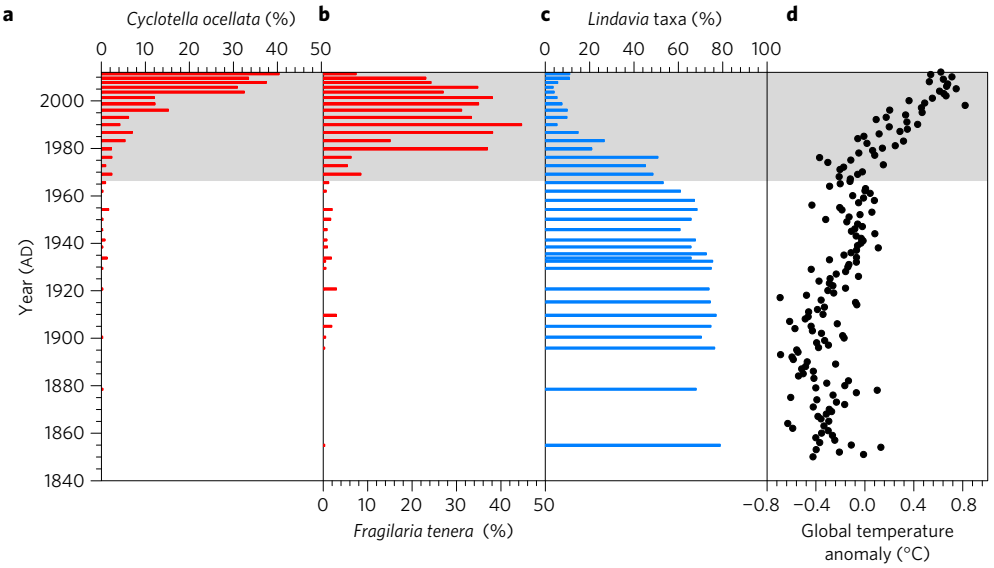

Figure 3 | The major shift in diatom assemblage composition recorded in the Lake Gonghai sediment core (GH13F) compared to the global mean air temperature trend observed during the anthropogenic warm period. a–c, The relative abundances of diatom taxa represented by a rise to dominance of *Cyclotella ocellata* (**a**) and *Fragilaria tenera* (**b**), well-documented indicators of warming (that is, decreasing ice cover, extended thermal stratification[6]), and a concurrent decline (**c**) in *Lindavia* taxa (*L. praetermissa and L. bodanica*), diatoms characteristic of low nutrients in alpine environments. **d**, Global mean temperature change[9], which is strongly correlated with the temperature change over the past 55 years observed in the meteorological observation station in the Lake Gonghai region ($R = 0.89$; $P < 0.001$; d.f. $= 55$). The shaded area represents a pronounced increase in air temperature during the past few decades.

over several years within each sedimentary core interval, thereby incorporating within-lake seasonal changes, including fluctuations in nutrient distributions as a result of vertical mixing and thermal stratification. Here, we use a long (3.96 m) sediment core (GH09B) dated using ^{14}C geochronology (Supplementary Fig. 2; see Methods) to focus on diatom responses (~25 years/interval) to known warming periods over the past ~2,000 years (Fig. 2), whereas we use a shorter core (GH13F) with chronology established using ^{210}Pb gamma spectroscopy (Supplementary Fig. 3; see Methods) to track high-resolution (~4 years/interval) diatom responses to current warming-related environmental changes within the context of the past ~175 years (Fig. 3).

Palaeoecological records from the past ~2,000 years have clearly documented two warm periods throughout China, consisting of the Sui–Tang Warm Period (STWP, AD 541–760) during the Sui–Tang dynasties, and the Medieval Warm Period (MWP, AD 931–1320), which broadly corresponds to the Song–Yuan dynasties[5]. These past warm periods were associated with strong Asian summer monsoons with abundant rainfall and greater wind intensity, as warming typically results in a sharper land/ocean thermal contrast[23–26] (Fig. 2b). These warm periods with strong summer monsoons are clearly expressed in our diatom records from the CLP (Fig. 2 and Supplementary Fig. 4). For example, a sharp increase in temperature during the Sui–Tang Warm Period—STWP (AD 541–760) and the Medieval Warm Period—MWP (AD 931–1320) resulted in abrupt and nearly complete shifts in diatom species dominance from low nutrient *Lindavia* taxa (*L. praetermissa and L. bodanica*) to eutrophic *Stephanodiscus hantzschii* (Supplementary Fig. 4). *S. hantzschii* is an unambiguous indicator of high phosphorus (P) levels, whereas *Lindavia* taxa are often associated with lower nutrients in alpine environments[27]. Pronounced shifts in dominance between oligotrophic (Fig. 2e) and eutrophic taxa (Fig. 2d) are synchronous with temperature reconstructions in North China based on 2,000 years of historical documents of phenological observations, including variations in regional flowering[5,28] (Fig. 2a), and have strong temporal coherence with the summer monsoon rainfall record[24–26] (Fig. 2b) and the sediment phosphorus record

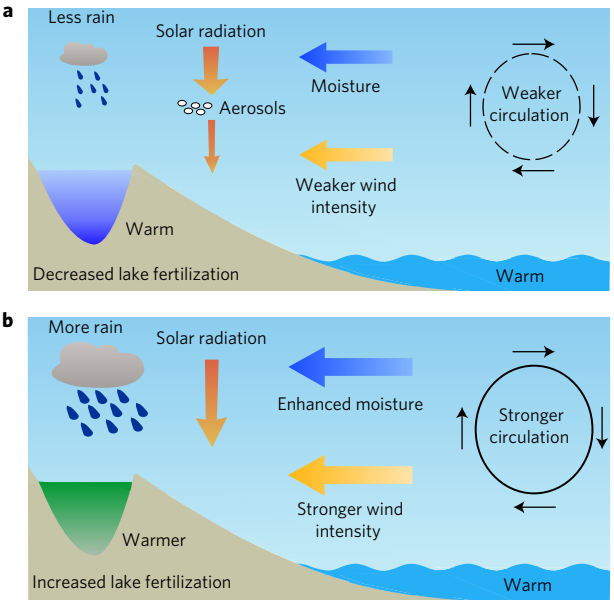

Figure 4 | Schematic diagram illustrating the different ecosystem responses to recent anthropogenic and past warming in monsoon regions. **a**, Recent anthropogenic warming period: aerosol-weakened summer monsoons decrease lake fertilization. Atmospheric aerosol loading decreases the amount of incoming solar radiation by scattering/absorbing the solar radiation in the atmosphere, resulting in slower surface warming over land and a reduction in the land–sea temperature contrast, which thus weakens the strength and extent of the overall monsoon circulation. This results in decreased monsoon rainfall and wind intensity from the ocean to land, which lessens erosion and decreases lake fertilization. **b**, Previous warming periods: warming led to strengthened summer monsoons, resulting in increased lake fertilization. Natural warm periods in the past were associated with a higher land/ocean thermal contrast, resulting in stronger summer monsoon circulation with an increase in summer monsoon rainfall and wind intensity that led to increased lake fertilization.

(Fig. 2c). These sedimentary records indicate that the STWP and MWP in the CLP were accompanied with strong summer monsoons and increased rainfall intensity that resulted in the transport of large quantities of phosphorus-rich soil eroded from the surrounding catchment, leading to marked natural lake fertilization.

In addition to increased P supplied from eroded catchment soil, an increase in summer monsoon wind strength during the STWP and MWP would also increase the duration and strength of water column mixing, enhancing internal nutrient recycling[29] and favouring dominance by eutrophic diatom taxa (Fig. 2d). In contrast, periods of dominance by oligotrophic diatom taxa (Fig. 2e) during cooler periods, such as the Little Ice Age, are associated with weaker summer monsoon rainfall intensity and wind strength, resulting in diminished delivery of phosphorus-rich soil, and thus lower water nutrient concentrations.

In contrast to past warm periods experienced in the CLP, anthropogenic warming over the past half century has initiated vastly different but equally pronounced responses that are well expressed in our palaeolimnological records (Fig. 3 and Supplementary Fig. 5). The most recent warm period, commencing around the 1960s, tracks a nearly complete shift in species dominance from large-celled and heavier *Lindavia* taxa (*L. praetermissa*, *L. bodanica*) (Fig. 3c) to the abrupt arrival and dominance of more buoyant *Cyclotella ocellata* and *Fragilaria tenera* (Fig. 3a,b) for the first time in the ~2,000-year sedimentary record (Supplementary Fig. 4). These shifts among diatom taxa with similar nutrient optima, but different ecophysiological traits, are consistent with the rise in mean temperatures (Fig. 3d) and concomitant increases in thermal stability and attendant changes in resource availability[6]. The most recent diatom shifts are indicative of a fundamentally different climate mechanism and biological response from the previous STWP and MWP warm episodes.

The acceleration of aerosol emissions, as a result of rapid industrialization in Asia over the past few decades, compounded by a lack of strict air pollution control, has resulted in Asia being a major contributor to twentieth-century anthropogenic climate forcing. Anthropogenic aerosols have increased cloud albedo and heightened scattering of incoming solar radiation back to space, resulting in slower surface warming over land and a reduction in the thermal contrast between the Asian continent and the adjacent ocean basins at decadal timescales[15,16] (Fig. 4). As such, anthropogenic aerosol forcings have been shown to weaken Asian summer monsoon rainfall and wind intensity over the past 50 years[1,13–16] (Fig. 2b), which explains why the Current Warm Period (CWP) is warmer than the MWP but precipitation is lower[17]. We demonstrate that this has resulted in a marked decline in the delivery of phosphorus-rich soil from the CLP (Fig. 2c) that is consistent with the decreasing trend in inter-annual rainfall variability[10] and, as recorded in the diatom assemblages, with a fundamental ecological change in aquatic ecosystems that includes a decline in lake nutrients and an increase in thermal stability.

Anthropogenic aerosols have fundamentally reversed the key limnological effects of warming on summer monsoon intensity and aquatic ecosystem properties (trophic status, mixing), highlighting that past climate is a poor analogue for recent warming and future climate trajectories in this economically and environmentally important region. The aerosol-affected period of recent anthropogenic warming has resulted in markedly different (albeit predictable) responses in lake ecosystem properties, hitherto not recorded in the previous two millennia. The consequences of these changes will undoubtedly cascade throughout the ecosystem. Ironically, continued environmental efforts to decrease anthropogenic aerosols in Asia, whilst global warming continues, will lead to the return of severe eutrophication, further impairing the already stressed freshwater supply of the region.

Methods

Methods, including statements of data availability and any associated accession codes and references, are available in the online version of this paper.

Received 12 September 2016; accepted 6 January 2017; published online 27 February 2017

References

1. Yu, S. *et al*. Anthropogenic aerosols are a potential cause for migration of the summer monsoon rain belt in China. *Proc. Natl Acad. Sci. USA* **113,** E2209–E2210 (2016).
2. Bollasina, M. A., Ming, Y. & Ramaswamy, V. Anthropogenic aerosols and the weakening of the South Asian summer monsoon. *Science* **334,** 502–505 (2011).
3. Menon, S., Hansen, J., Nazarenko, L. & Luo, Y. Climate effects of black carbon aerosols in China and India. *Science* **297,** 2250–2253 (2002).
4. Yan, Q., Zhang, Z., Wang, H. & Jiang, D. Simulated warm periods of climate over China during the last two millennia: the Sui–Tang warm period versus the Song–Yuan warm period. *J. Geophys. Res.* **120,** 2229–2241 (2015).
5. Ge, Q., Zheng, J., Hao, Z. & Liu, H. General characteristics of climate changes during the past 2000 years in China. *Sci. China Earth Sci.* **56,** 321–329 (2013).
6. Rühland, K. M., Paterson, A. M. & Smol, J. P. Lake diatom responses to warming: reviewing the evidence. *J. Paleolimnol.* **54,** 1–35 (2015).
7. Liu, T. *Loess and the Environment* (China Ocean, 1985).
8. Fu, B. J. Soil erosion and its control in the Loess Plateau of China. *Soil Use Manage.* **5,** 76–82 (1989).
9. IPCC *Climate Change 2013: The Physical Science Basis* (eds Stocker, T. F. *et al.*) (Cambridge Univ. Press, 2013).
10. Xin, Z., Yu, X., Li, Q. & Lu, X. X. Spatiotemporal variation in rainfall erosivity on the Chinese Loess Plateau during the period 1956–2008. *Reg. Environ. Change* **11,** 149–159 (2011).
11. Tao, Y., Wei, M., Ongley, E., Li, Z. & Jingsheng, C. Long-term variations and causal factors in nitrogen and phosphorus transport in the Yellow River, China. *Estuar. Coast Shelf Sci.* **86,** 345–351 (2010).
12. Liu, J. & Diamond, J. China's environment in a globalizing world. *Nature* **435,** 1179–1186 (2005).
13. Xu, M. *et al*. Steady decline of East Asian monsoon winds, 1969–2000: evidence from direct ground measurements of wind speed. *J. Geophys. Res.* **111,** D24111 (2006).
14. Li, X. Q., Ting, M., Li, C. H. & Henderson, N. Mechanisms of Asian summer monsoon changes in response to anthropogenic forcing in CMIP5 models. *J. Clim.* **28,** 4107–4125 (2015).
15. Salzmann, M., Weser, H. & Cherian, R. Robust response of Asian summer monsoon to anthropogenic aerosols in CMIP5 models. *J. Geophys. Res.* **119,** 11321–11337 (2014).
16. Song, F., Zhou, T. & Qian, Y. Responses of East Asian summer monsoon to natural and anthropogenic forcings in the 17 latest CMIP5 models. *Geophys. Res. Lett.* **41,** 596–603 (2014).
17. Liu, J., Wang, B., Cane, M. A., Yim, S. Y. & Lee, J. Y. Divergent global precipitation changes induced by natural versus anthropogenic forcing. *Nature* **493,** 656–659 (2013).
18. Smith, D. M. *et al*. Role of volcanic and anthropogenic aerosols in the recent global surface warming slowdown. *Nat. Clim. Change* **6,** 936–940 (2016).
19. Lu, C. & Tian, H. Half-century nitrogen deposition increase across China: a gridded time-series data set for regional environmental assessments. *Atmos. Environ.* **97,** 68–74 (2014).
20. Wang, Q., Fan, X. & Wang, M. Recent warming amplification over high elevation regions across the globe. *Clim. Dynam.* **43,** 87–101 (2014).
21. Mountain Research Initiative EDW Working Group. Elevation-dependent warming in mountain regions of the world. *Nat. Clim. Change* **5,** 424–430 (2015).
22. Hall, R. I. & Smol, J. P. *The Diatoms: Applications for the Environmental and Earth Sciences* (eds Smol, J. P. & Stoermer, E. F.) 122–151 (Cambridge Univ. Press, 2010).
23. Chen, J. H. *et al*. Hydroclimatic changes in China and surroundings during the medieval climate anomaly and Little Ice Age: spatial patterns and possible mechanisms. *Quat. Sci. Rev.* **107,** 98–111 (2015).
24. Zhang, P. Z. *et al*. A test of climate, sun, and culture relationships from an 1810-year Chinese cave record. *Science* **322,** 940–942 (2008).
25. Tan, L. *et al*. Centennial-to decadal-scale monsoon precipitation variability in the semi-humid region, northern China during the last 1860 years: records from stalagmites in Huangye Cave. *Holocene* **21,** 287–296 (2011).
26. Liu, J., Wang, B., Wang, H., Kuang, X. & Ti, R. Forced response of the East Asian summer rainfall over the past millennium: results from a coupled model simulation. *Clim. Dynam.* **36,** 323–336 (2011).

27. Yang, J. R., Pick, F. R. & Hamilton, P. B. Changes in the planktonic diatom flora of a large mountain lake in response to fertilization. *J. Phycol.* **32,** 232–243 (1996).
28. Ge, Q. S. *et al*. Winter half-year temperature reconstruction for the middle and lower reaches of the Yellow River and Yangtze River, China, during the past 2000 years. *Holocene* **13,** 933–940 (2003).
29. Bracht, B. B., Stone, J. R. & Fritz, S. C. A diatom record of late Holocene climate variation in the northern range of Yellowstone National Park, USA. *Quat. Int.* **188,** 149–155 (2008).
30. Yi, S. *Holocene Vegetation Responses to East Asian Monsoonal Changes in South Korea* (INTECH Open Access Publisher, 2011).
31. Fu, B. J. *et al*. Assessing the soil erosion control service of ecosystems change in the Loess Plateau of China. *Ecol. Complexity* **8,** 284–293 (2011).

Acknowledgements

We thank members of the Paleoecological Environmental Assessment and Research Laboratory and G. J. Chen for their help with the laboratory analyses; S. Kandasamy, Z. L. Wang, L. Lin, M. R. Qiang, G. H. Dong, Y. L. Li, X. S. Zhang and Y. Li for critical discussions and reading of the manuscript; X. J. Zhang and Z. P. Zhang for assistance in figure preparation; and Z. L. Wang, X. Y. Cao and Y. C. Li for fieldwork, respectively. This work was supported by the National Natural Science Foundation of China (No. 41601186, 41130102, 41471162 and 41505043), Fundamental Research Funds for the Central Universities (No. lzujbky-2016-155), and the Natural Sciences and Engineering Research Council of Canada to J.P.S.

Author contributions

J.P.S. and F.C. designed this study. J.P.S., J.L., K.M.R. and F.C. led the interpretation and writing. Q.X. and J.C. organized field work. J.P.S., K.M.R. and J.L. led the diatom analysis. J.L., K.M.R. and J.P.S. performed diatom analysis. J.L. and J.C. performed geochemical data analysis. J.L., K.M.R. and F.C. constructed the age-depth model. J.L., J.P.S., K.M.R., Y.X., J.C., S.C., F.C., Q.C. and H.W. wrote the manuscript. All authors discussed the results and provided input to the manuscript.

Additional information

Supplementary information is available in the online version of the paper. Reprints and permissions information is available online at www.nature.com/reprints. Correspondence and requests for materials should be addressed to F.C. or J.P.S.

Competing financial interests

The authors declare no competing financial interests.

Methods

Field sampling and analytical methods. We collected two sediment cores (a long core and a short core) from the alpine Lake Gonghai. The long core (GH09B) was obtained from the centre of the lake (Supplementary Fig. 1) in January of 2009 using an Uwitec Piston Corer. It was sub-sampled at 1-cm intervals, and we focus on the uppermost fine-grained lacustrine sediments (3.96 m), which spans approximately the past 2,000 years. The chronology was established using accelerator mass spectrometry (AMS) ^{14}C dating of seven terrestrial plant macrofossils samples. Supplementary Table 1 lists the measured and calibrated ages[32]. The ages are expressed in years before present (BP), where 'present' is defined as AD 1950. Bayesian age–depth modelling performed using OxCal v4.2.2 and a Poisson-process (P-sequence) single depositional model at 1-cm increments with a K value of 100 (ref. 33) was used to produce the age-depth model (Supplementary Fig. 2).

The short core (GH13F), 57.5 cm in length, was obtained from the deepest part of Lake Gonghai (Supplementary Fig. 1) in August 2013 using a Universal gravity corer (internal core tube diameter = 6.8 cm) and sectioned on-site using a close-interval extruder into 0.5-cm intervals. The chronology of this high-resolution surface sediment core for the past ~175 years (Supplementary Fig. 3) was established using a constant-rate-of-supply (CRS) model applied to excess ^{210}Pb inventories, counted on a digital, high-purity germanium γ spectrometer (DSPec, Ortec), following standard gamma counting procedures[34].

For both cores, diatom preparations followed standard protocols for siliceous microfossils[35]; at least 300 diatom valves were identified and enumerated per interval. Diatom analysis was undertaken on a total of 78 samples from the uppermost part of the GH09B core (3.96 m) with an average temporal resolution of ~25 years and on 38 samples from the GH13F core (0.57 m) with an average temporal resolution of ~4 years.

To estimate the amount of soil phosphorus eroded from the CLP, we measured the phosphorus concentration of bulk sediments from core GH09B over the past 2,000 years. Concentrations of sedimentary phosphorus were determined with an X-ray fluorescence (XRF) spectrometer (PANalytical PW2403/00) equipped with a super sharp tube for the Rh-anode, with the following settings: 4 kW, 60 kV, 160 mA and a 75 μUHT Be end window. The company's SuperQ software (version 5) was used for the calculation.

Data availability. The data generated and analysed during the current study (diatom relative abundances, sediment phosphorus concentrations) that support the findings of this publication are available from the corresponding authors on request. Radioisotopic dating data generated and/or analysed during the current study are included in this published article (and its Supplementary Information files).

References

32. Liu, J. B. *et al*. Humid Medieval Warm Period recorded by magnetic characteristics of sediments from Gonghai Lake, Shanxi, North China. *Chin. Sci. Bull.* **56,** 2464–2474 (2011).
33. Ramsey, C. B. Deposition models for chronological records. *Quat. Sci. Rev.* **27,** 42–60 (2008).
34. Appleby, P. G. in *Tracking Environmental Change using Lake Sediments-Volume 1: Basin Analysis, Coring, and Chronological Techniques* (eds Last, W. M. & Smol, J. P.) 171–203 (Springer, 2001).
35. Battarbee, R. W. *et al*. in *Tracking Environmental Change using Lake Sediments-Volume 3: Terrestrial, Algal, and Siliceous Indicators* (eds Smol, J. P., Birks, H. J. B. & Last, W. M.) 155–202 (Springer, 2001).

nature climate change

SUPPLEMENTARY INFORMATION

DOI: 10.1038/NCLIMATE3220

In the format provided by the authors and unedited.

Aerosol-weakened summer monsoons decrease lake fertilization on the Chinese Loess Plateau

Jianbao Liu[1,2], Kathleen M. Rühland[3], Jianhui Chen[1], Yangyang Xu[4], Shengqian Chen[1], Qiaomei Chen[1], Wei Huang[1], Qinghai Xu[5], Fahu Chen[1,2]* and John P. Smol[3]*

[1]Key Laboratory of West China's Environmental System (Ministry of Education), College of Earth and Environmental Sciences, Lanzhou University, Lanzhou 730000, China. [2]CAS Center for Excellence in Tibetan Plateau Earth Sciences of the Chinese Academy of Sciences, Beijing 100101, China. [3]Paleoecological Environmental Assessment and Research Lab (PEARL), Department of Biology, Queen's University, Kingston, Ontario, K7L 3N6, Canada. [4]Department of Atmospheric Science, Texas A&M University, College Station, Texas 77842, USA. [5]Institute of Nihewan Archaeology Research College of Resources and Environment, Hebei Normal University, Shijiazhuang 050024, China. *e-mail: fhchen@lzu.edu.cn; smolj@queensu.ca

16 **Supplementary Figures**

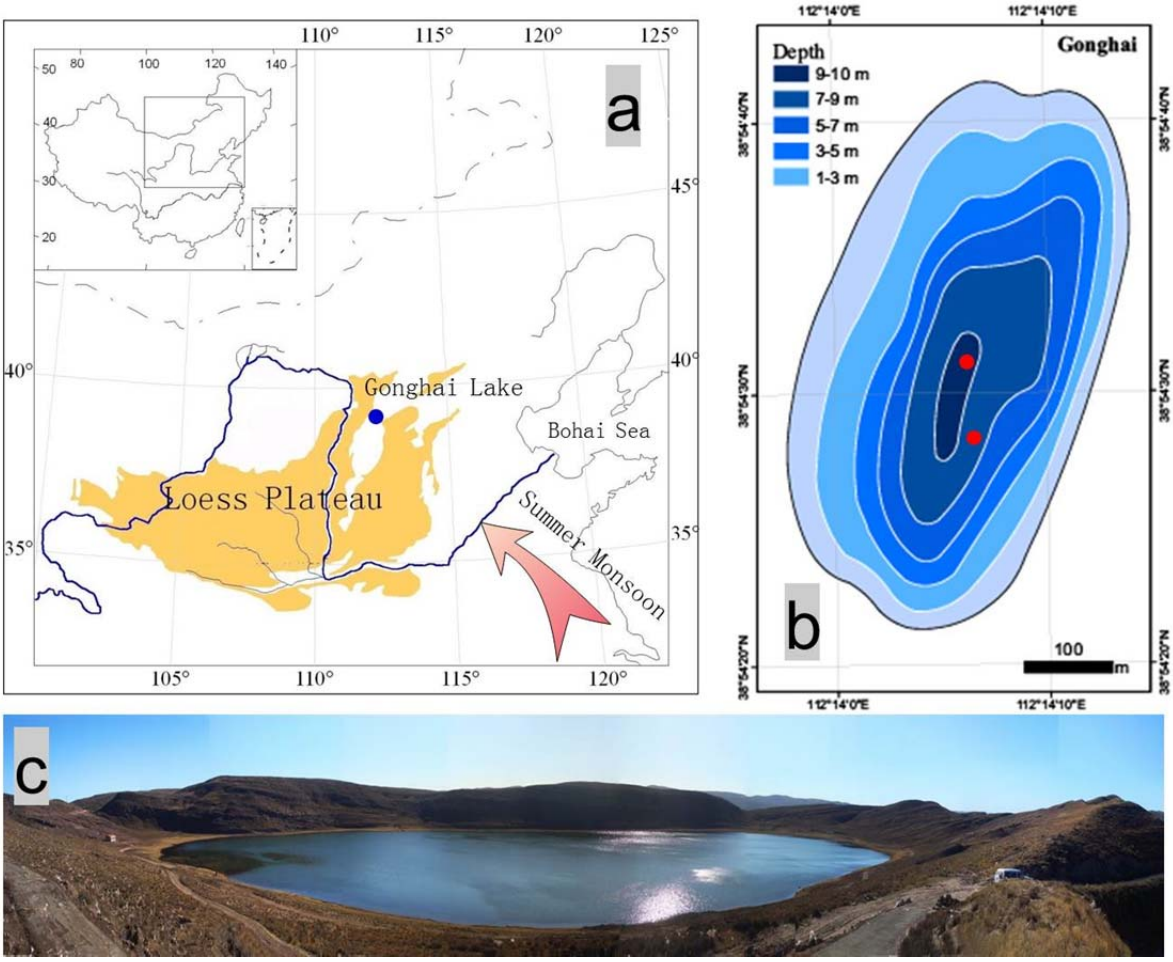

17

18 **Figure S1 | Location and settings.** (**a**) Location of Lake Gonghai (blue circle) in the Chinese
19 Loess Plateau. The Yellow River (blue line) and the dominant circulation system (arrows) of the
20 Asia summer monsoon are also shown. (**b**) Bathymetry of Lake Gonghai. The red dots indicate
21 the location of the Lake Gonghai sediment cores. (**c**) Photograph of Lake Gonghai and its
22 catchment.

23

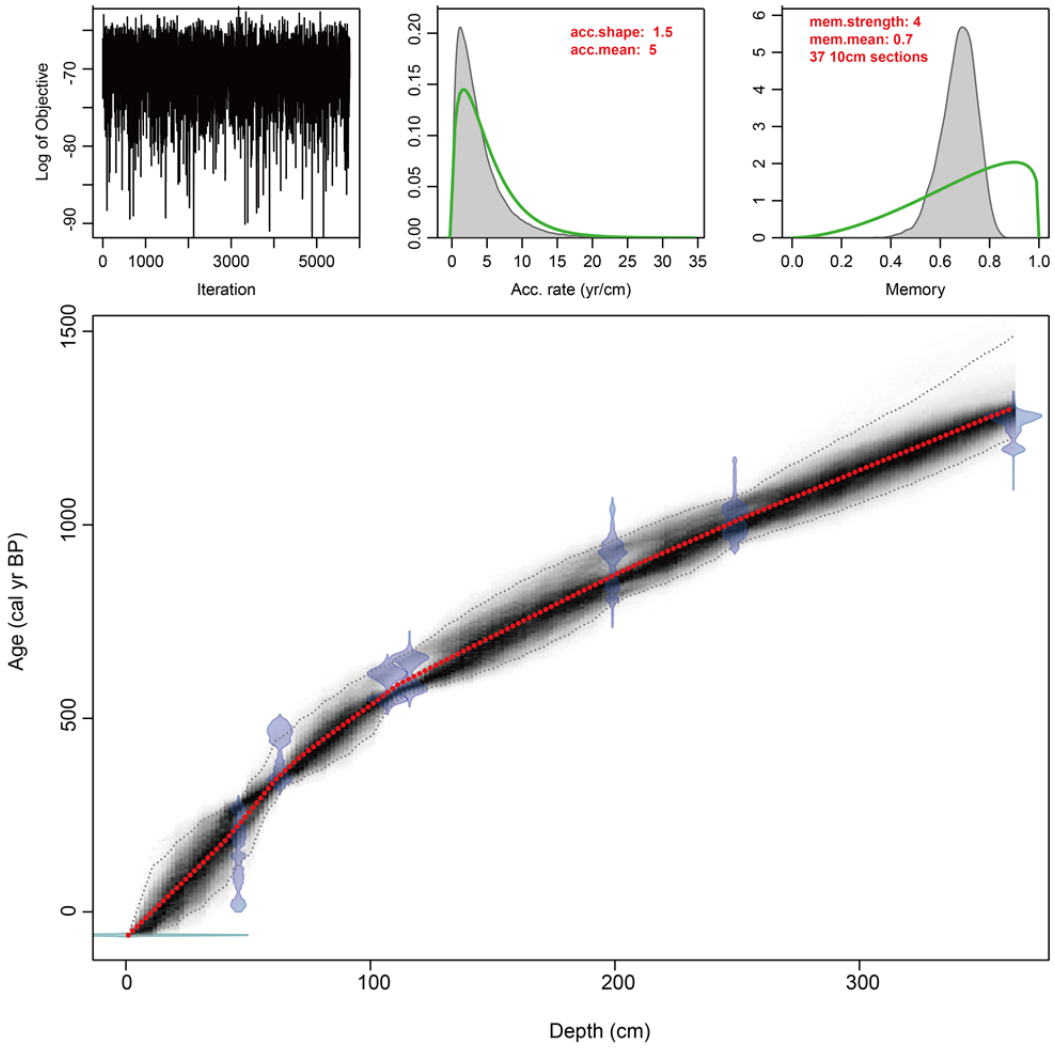

Figure S2 | Age-depth model for the Lake Gonghai sediment core (GH09B) over the past 2000 years. Upper panels depict the Markov Chain Monte Carlo (MCMC) iterations (left; good runs show a stationary distribution with little structure among neighbouring iterations), the prior (green curves) and posterior (grey histograms) distributions for the accumulation rate (middle panel) and memory (right panel). The bottom panel shows the calibrated ^{14}C dates (transparent light blue) and the age-depth model (darker greys indicate most probable calendar ages; grey stippled lines represent 95% confidence intervals; red curve shows single 'best' model based on the weighted mean age for each depth interval).

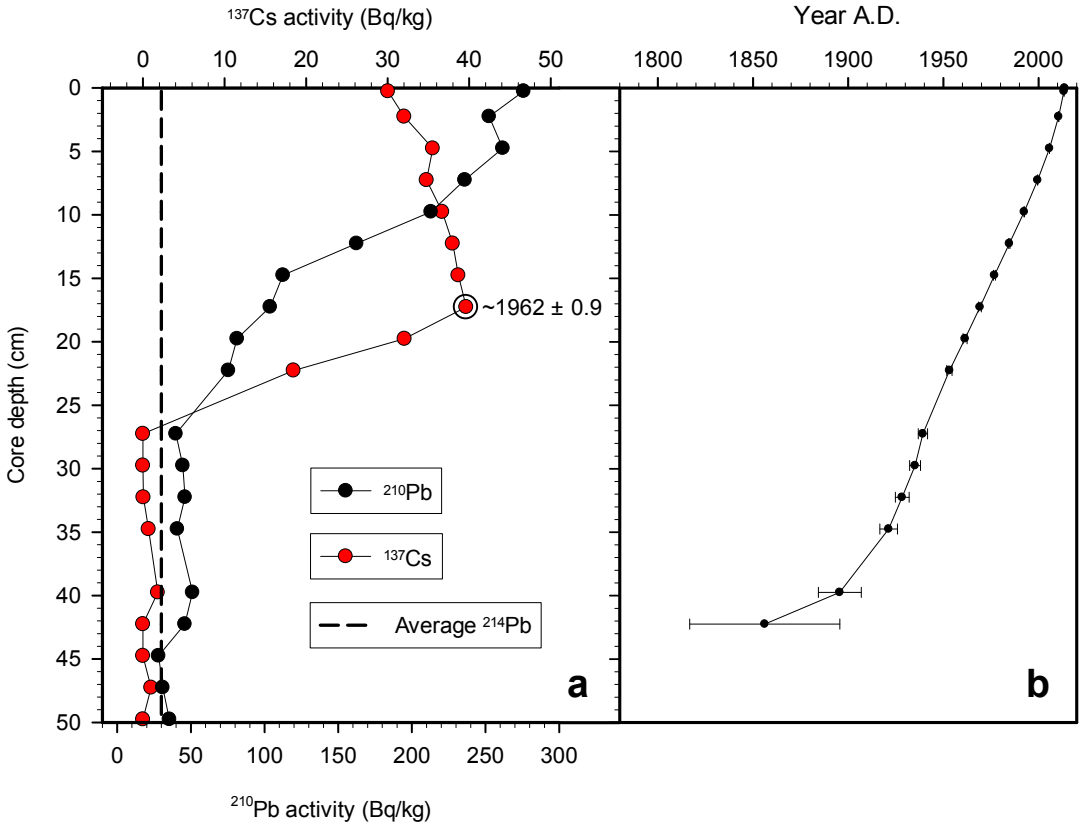

Figure S3 | Age-depth model for the Lake Gonghai surface sediment core (GH13F) over the past ~150 years. Radiometric dating analysis using gamma spectroscopy showing (**a**) ^{210}Pb, ^{214}Pb, and ^{137}Cs activities in becquerels per kilogram (Bq/kg) dried sediment plotted against core depth, and (**b**) estimated age (A.D.) plotted against core depth and associated errors based on the constant rate of supply (CRS) model. The dashed vertical line in (a) is the mean of all sample-specific ^{214}Pb activities counted in the core and is a proxy for supported ^{210}Pb. The CRS date of 1962 ± 0.9 associated with the interval of highest ^{137}Cs activity depicted in (**a**) is an excellent match with the height of nuclear fallout resulting from the 1963 global moratorium on weapons testing, further confirming the veracity of the ^{210}Pb dating chronology.

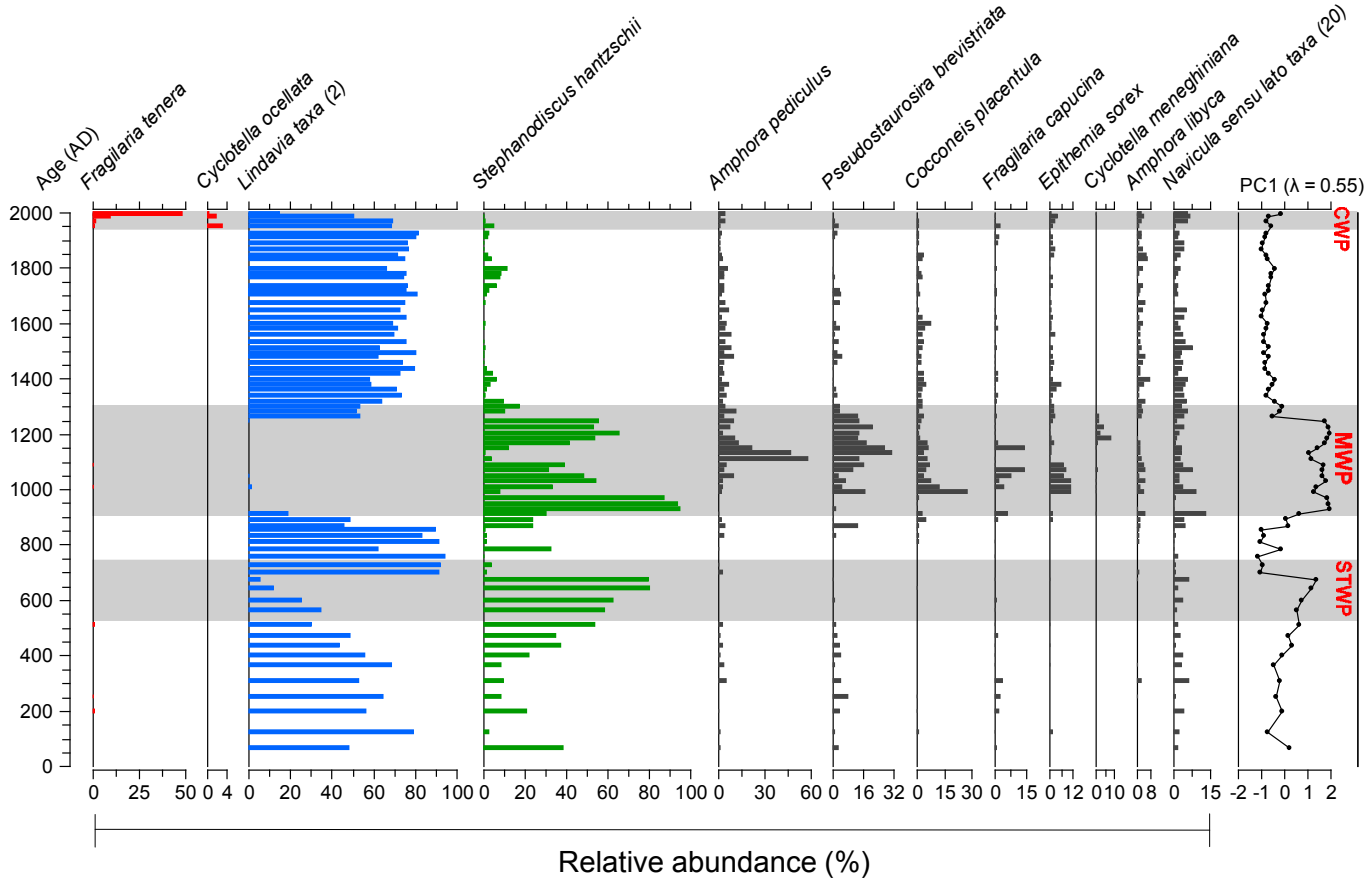

Figure S4 | Stratigraphic profile showing the relative abundances of the most common diatom taxa from Lake Gonghai (core GH09B), as well as the PCA axis 1 sample scores of the diatom assemblages. Some diatom taxa have been grouped for clarity and the number of taxa in each group is indicated in parentheses. The dominant oligotrophic *Lindavia* taxa (*L. praetermissa and L. bodanica*) and eutrophic *Stephanodiscus hantzschii* are presented in blue and green, respectively. The shaded areas represent the Sui-Tang Warm Period (STWP), the Medieval Warm Period (MWP), and the Current Warm Period (CWP). Cluster analysis using constrained incremental sum of squares (CONISS) with Euclidean squared distances as the measure of dissimilarity generated in TGView v. 1.7.16[1] determined that stratigraphic zones (dendrogram not shown) matched the timing of high magnitude diatom responses to the three warm periods. λ represents the associated eigenvalue for the PCA axis 1 sample scores.

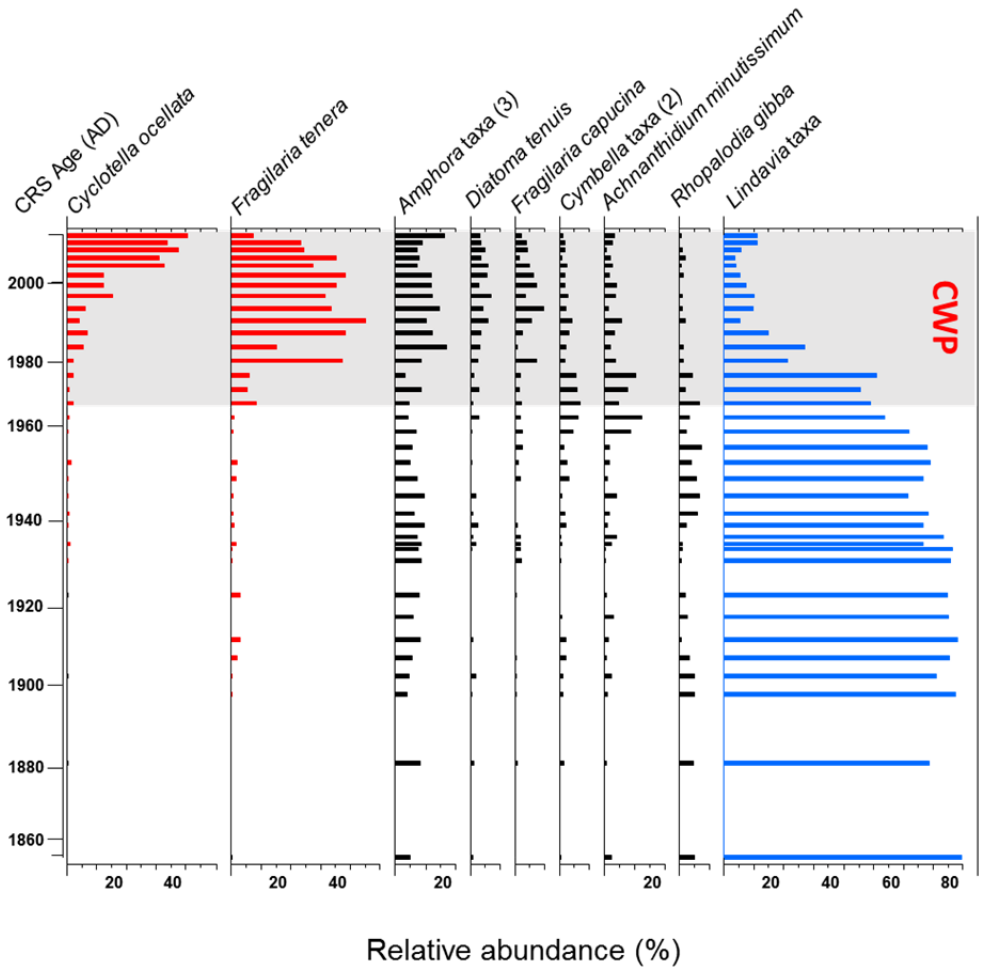

Figure S5 | Stratigraphic profile showing the percent relative abundances of the most common diatom taxa (occurring at 5% in at least 4 intervals) from the Lake Gonghai short core (GH13F). Certain genera were grouped for clarity and the number of taxa in each group are indicated in parentheses (e.g. *Amphora* and *Cymbella*). The shaded area represents a pronounced increase in regional and global mean air temperature during the Current Warm Period (CWP). Cluster analysis using constrained incremental sum of squares (CONISS) with Euclidean squared distances as the measure of dissimilarity generated in TGView v. 1.7.16[1] determined that the main stratigraphic zones (dendrogram not shown) matched the timing of high magnitude diatom responses during the CWP.

Supplementary Table

Table S1 Radiocarbon dates of terrestrial plant-macrofossil samples used to construct the chronology for core GH09B from Lake Gonghai.

Lab ID	Sample No.	Depth (cm)	Material	$\delta^{13}C$ ‰	Conventional Age (1σ, BP yr)	Calibrated Age(1σ, Cal yr BP)
Beta306751	GHB1-35	46	Stem	-25.9	150±30	0-282
XA4667	GHB1-48	63	Leaf	-24.9	368±23	332-498
XA5587	GHB1-82	107	Leaf	-15.7	570±25	540-628
XA4669	GHB1-89	116	Stem	-30.7	665±34	565-668
XA4670	GHB1-153	199	Stem	-30.9	1005±40	804-963
XA4668	GHB1-191	249	Stem	-30.4	1102±30	968-1053
XA4671	GHB2-76	363	Stem	-25.4	1329±25	1194-1294

References

1. Grimm, E. C. CONISS: a Fortran 77 program for stratigraphically constrained cluster analysis by the method of incremental sum of squares. *Comput. Geosci.* **13**, 13–35 (1987).